







DC-Bus Signaling Control Laws for the Operation of DC-Microgrids With Renewable Power Sources

Iván Patrao , Enric Torán , Raúl González-Medina , Marian Liberos , Emilio Figueres , *Senior Member, IEEE*, and Gabriel Garcerá , *Senior Member, IEEE*

Abstract—DC-bus signaling (DBS) is a proven method to coordinate different microgrid agents, using the dc voltage of the microgrid as a communication signal. The droop control applied in a dc microgrid achieves accurate power-sharing among converters while leading to a certain voltage regulation error in the microgrid bus. The behavior of the different agents in a microgrid is managed by using the voltage at each node of the microgrid as the DBS signal. The technique proposed in this article uses an improved DBS technique to coordinate interlinking converters, photovoltaic generators, energy storage systems (ESSs), and loads in a microgrid. The operation of the renewable power sources of a microgrid at the full generated power is desired due to economic and environmental reasons. The DBS technique proposed in this article is adapted to integrate renewable power sources in the microgrid. The DBS-controlled ESSs will store the surplus energy if the generated power exceeds consumption. In the case of fully charged ESS, the renewable generators will limit their output power to those demanded by the loads. The proposed control laws have been tested in an experimental microgrid.

Index Terms—DC-bus signaling (DBS), dc-bus, droop, load, management, microgrids, power, sharing.

I. INTRODUCTION

COOPERATION of small-scale generators (renewable or not) and mid/big-scale generators forming a microgrid is the new paradigm in energy management [1], [2], [3]. The microgrid performance can be boosted by dynamic load management [4], [5] in coordination with energy storage systems (ESS) [6]. Intelligent control of generators, loads, and storage systems leads to excellent grid quality, reliability, and lower exploitation costs and CO₂ emissions.

A microgrid has different agents distributed among a physical area (generators, ESS, and loads). However, these agents must work together to operate the microgrid within the desired parameters of robustness and stability [7], [8]. The coordination

system often uses communication links between the agents in a microgrid, but they are a critical issue due to costs, delays, and reliability [8]. Hence, communication links should be avoided if it is possible. Otherwise, low-speed fault-tolerant communication links should be used [9], [10].

Microgrid generators frequently use the droop control technique [11]. However, the operation of distributed generators under droop laws leads to a degradation in voltage accuracy. Moreover, power-sharing among the different converters in the microgrid is a critical issue. Consequently, many papers dealing with communications have been published to reduce voltage error and improve load-sharing accuracy [12].

Since the communication links increase the cost and reduce the reliability of the overall system, the operation based on terminal values (i.e., dc voltage of the microgrid) of the agents of the microgrid is desired. In the dc-bus signaling (DBS) method, the agents adjust their operation mode based on their own terminals' voltage value. The DBS method often coordinates the different types of generators and loads in dc microgrids [13], [14], [15].

In the literature, it is possible to find various proposals for secondary control [16] using the bus voltage to coordinate the operating mode and power-sharing in dc microgrids. A voltage-level signaling (VLS) technique has been proposed in [14] and [17]. In this method, the voltage variation of the dc-bus is divided into windows, each assigned to specific operating modes. It is a cheap and easy-to-implement control method, but the achieved power-sharing is poor, and a vast number of paralleled converters may lead to excessive voltage windows. DBS is created by combining VLS and droop methods [18]. Hence, in DBS every change is progressive among operating states. Later, Sun et al. [19] presented an evolution of DBS called mode-selective DBS. The approach of this method is to decide which converter operates as a voltage source according to the dc-bus voltage, while the rest serve as current sources. Modifications with advanced features have been proposed recently [20], like communicative DBS, where voltage variations serve as a low-speed digital communication link.

Regarding VLS [14], [17], the technique proposed in this article uses a minimal number of voltage windows while providing a smooth behavior. To achieve this performance, several DBS control laws for the agents in a dc microgrid are proposed. Each control law fits the specific characteristics of the typical agents in a microgrid (interlinking converters, ESSs, and renewable energy sources). Compared with the mode-selective DBS [19], in the proposed technique all the generators behave as voltage

Manuscript received 7 July 2023; revised 1 November 2023; accepted 16 December 2023. Date of publication 22 December 2023; date of current version 12 July 2024. This work was supported by the Spanish “Ministerio de Asuntos Económicos y Transformación Digital” and the European Regional Development Fund (ERDF) under Grant RTI2018-100732-B-C21 and Grant PID2021-122835OB-C22. (*Corresponding autor: Iván Patrao.*)

The authors are with the Grupo de Sistemas Electrónicos Industriales del Departamento de Ingeniería Electrónica, Universitat Politècnica de València, 46022 Valencia, Spain (e-mail: ivpather@upvnet.upv.es; entomor@etsii.upv.es; raungome@upv.es; malimas@upv.es; efiguere@upvnet.upv.es; ggarcer@eln.upv.es).

Color versions of one or more figures in this article are available at <https://doi.org/10.1109/JESTIE.2023.3345797>.

Digital Object Identifier 10.1109/JESTIE.2023.3345797

sources, thus avoiding the master-slave or grid-forming/grid-following problems. Thus, a fully decentralized power-sharing algorithm performs the voltage regulation of the microgrid. Compared with the communicative DBS [20], no master module or communication links between agents are required. Thus, a plug-and-play dc microgrid is possible since any converter does not need to be informed about the characteristics of the rest of the converters.

Unlike frequency in ac systems, the node voltage is not a global measurement but a local parameter, providing information about the state of charge of each node. For instance, a low voltage stands for a highly loaded node, while a high voltage stands for a poorly loaded one.

The control technique proposed in this article proves to be a feasible method for the coordination and power management of renewable sources in a microgrid. The DBS control technique can coordinate the renewable generators and ESS devices to store the excess in production or limit the energy production in the case of fully charged ESS.

II. DC-BUS SIGNALING

The DBS method uses the dc bus voltage as a reliable parameter of the microgrid operating conditions. The voltage value measured at the output terminals of each converter determines the operating mode [14]. In the classical DBS method, the master converter usually establishes the microgrid dc voltage, and the rest of the converters in the microgrid operate according to this voltage level. For instance, the diesel generators in a microgrid will only work below a certain voltage level, remaining idle for voltages above that level. Some variations of this method have been presented [15].

Most dc buses are specified with a broad tolerance ratio since the agents connected to the microgrid have a dc/dc power converter with a wide input voltage range. In the DBS technique, such voltage error determines the operating mode of the agents in the microgrid.

The IEEE Standard 1547 limits the microgrid dc voltage variation between 0.95 and 1.05 p.u. For instance, the voltage of a 450 V_{DC} microgrid can swing between 427.5 V_{DC} and 472.5 V_{DC} under normal circumstances. Various published works try to use communication links to reduce this voltage error to very low values [21], but this is far beyond the objective of the standard.

The DBS technique takes advantage of this voltage deviation and uses it as a flag of the microgrid status. Moreover, due to the resistive behavior of the power transmission lines, the voltage of each node serves as an indicator of the node's state of load. Voltages near the highest limit (about 470 V_{DC}) suggest that this microgrid node drains only a small part of the available power. Voltages near the lower limit (about 430 V_{DC}) suggest that the load is close to the maximum node capacity. Thus, microgrid agents can decide how to act according to the voltage measured at their output (terminal values).

The 450 V_{DC} nominal value used in this work is in the range of the typical microgrid examples, but the results are independent

of the nominal value used in the tests. Hence, both low-voltage and high-voltage dc microgrids can implement this technique.

The linear behavior of the DBS technique can be modeled as (1), being P_{MAX} the nominal power of the converter, ΔP and ΔV the maximum variations of power and voltage, V_{NODE} the microgrid measured voltage, and V_{min} the minimum affordable voltage at this node. Since the DBS technique relies on the error deviation to adjust the output power reference, the measurement error in the voltage signal can affect the performance of the power-sharing technique. From (1), it can be derived the power perturbation (2) and the effect of the voltage deviations (3), where ΔV represents the node voltage variation, and V_{ERROR} is the measurement error in the voltage signal. Since the same coefficient ($\Delta P/\Delta V$) affects the error and voltage variations, its influence on the output power reference is similar. Hence, the DBS technique requires better accuracy of voltage sensing circuits than the nominal voltage variation

$$P_{REF} = P_{MAX} - \frac{\Delta P}{\Delta V} \cdot (V_{NODE} - V_{min}) \quad (1)$$

$$\Delta P_{REF} = \frac{-\Delta P}{\Delta V} \cdot (\Delta V) \quad (2)$$

$$\Delta P_{REF} = \frac{-\Delta P}{\Delta V} \cdot (\Delta V) + \frac{-\Delta P}{\Delta V} \cdot (V_{ERROR}). \quad (3)$$

Considering a microgrid formed by two converters of the same nominal power (P_N), delivering P_1 and P_2 output power, (4) and (5) are obtained. The influence of the voltage sensing error is represented in (5) as a voltage offset. Thus, the microgrid node voltage can be calculated as (6), where P_T represents the load power. The generalization of this equation for any number (N) of identical paralleled DBS-controlled converters leads to (7). Hence, it is demonstrated that the voltage error in the sensing circuits could significantly affect the power delivered by a converter. However, its effect on the voltage regulation of the entire microgrid is smaller as the number of converters increases

$$P_1 = P_N - \frac{\Delta P}{\Delta V} \cdot (V_{NODE} - V_{min}) \quad (4)$$

$$P_2 = P_N - \frac{\Delta P}{\Delta V} \cdot (V_{NODE} + V_{error} - V_{min}) \quad (5)$$

$$V_{NODE} = \left(P_N - \frac{P_T}{2} \right) \cdot \frac{\Delta V}{\Delta P} + \frac{V_{error}}{2} + V_{min} \quad (6)$$

$$V_{NODE} = \left(P_N - \frac{P_T}{N} \right) \cdot \frac{\Delta V}{\Delta P} + \frac{V_{error}}{N} + V_{min}. \quad (7)$$

III. PROPOSED CONTROL TECHNIQUE

The voltage swing of the microgrid dc voltage (from 430 V_{DC} to 470 V_{DC}) is divided into different working areas, as shown in Table I (microgrid nominal voltage: 450 V_{DC}). Minor voltage variations around its nominal value (± 10 V_{DC}) are considered mid-power operation mode: the generators have enough power to feed the loads. If the voltage falls below the -10 V_{DC} deviation, the microgrid generators still power the loads, but their output almost reaches its maximum capacity. If the loads demand more power, the microgrid generators will not be able to provide it.

TABLE I
MICROGRID VOLTAGE WORKING AREAS

Microgrid voltage	Description
$V_N - 20 \text{ V} < V_{\text{MICROGRID}} < V_N - 10 \text{ V}$ ($430 \text{ V}_{\text{DC}} < V_{\text{MICROGRID}} < 440 \text{ V}_{\text{DC}}$)	The power demanded by loads is almost equal to those available in generators.
$V_N - 10 \text{ V} < V_{\text{MICROGRID}} < V_N + 10 \text{ V}$ ($440 \text{ V}_{\text{DC}} < V_{\text{MICROGRID}} < 460 \text{ V}_{\text{DC}}$)	Mid power operation
$V_N + 10 \text{ V} < V_{\text{MICROGRID}} < V_N + 20 \text{ V}$ ($460 \text{ V}_{\text{DC}} < V_{\text{MICROGRID}} < 470 \text{ V}_{\text{DC}}$)	A great amount of available power is in the generators.

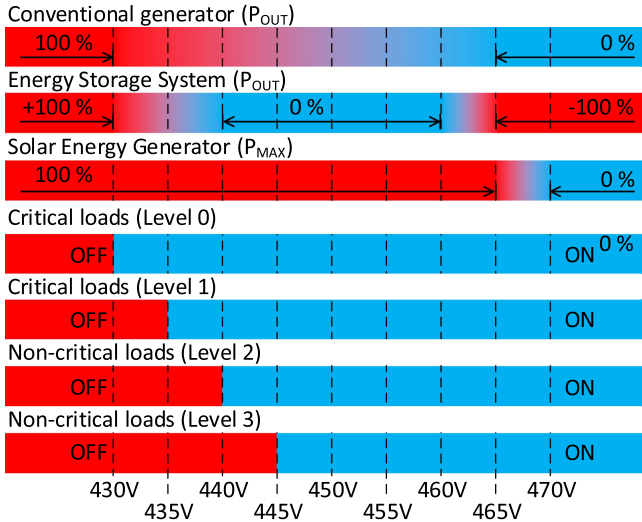


Fig. 1. DBS trip voltage values (nominal voltage: $450 \text{ V}_{\text{DC}}$).

On the contrary, if the voltage exceeds the $+10 \text{ V}_{\text{DC}}$ deviation, the microgrid has light-load conditions, and the generators have significant available power.

In this work, the control algorithm of each converter calculates the power to be delivered using the node voltage measurement. This technique leads to a wireless power-sharing behavior. Moreover, the microgrid dc voltage is used to adjust the operating mode of some converters; for instance, the ESS charges the battery for high voltage values and discharges the battery to provide power support for low voltage values. We present control laws for interlinking converters, photovoltaic (PV) power sources, and ESS. Moreover, the loads use this node voltage value to decide whether they must remain connected or be disconnected to prevent the collapse of the microgrid. The definition of four different priority levels will determine the management of such loads. The trip voltage values proposed in this article are shown in Fig. 1, which are established so that the performance of each agent is optimized to reinforce the microgrid’s stability. The behavior of any type of agent is based on those presented in [22], but in the following sections, it is revised and complemented.

When some generators lose their power capacity, the DBS load-managing technique disconnects the loads based on their priority, adapting the consumption to the available power. So, the loss of any generator’s capacity is not a critical issue since

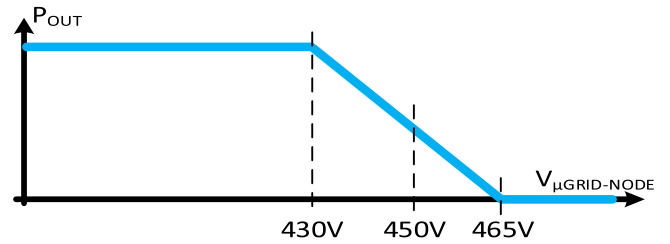


Fig. 2. DBS control law for interlinking converters.

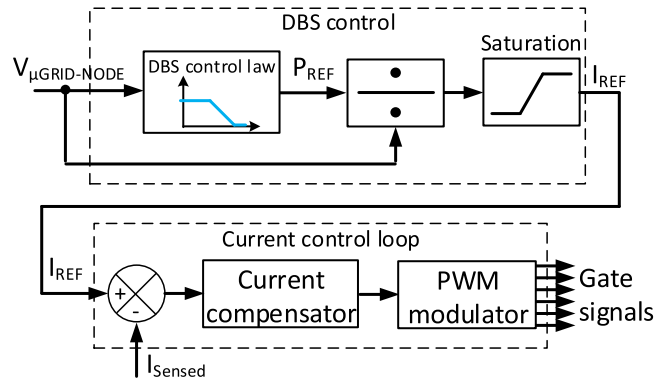


Fig. 3. Power control loop based on DBS.

the worst scenario leads to the disconnection of loads based on a prioritized level of importance.

A. Interlinking Converters

The interlinking converters, seen in the dc-microgrid as dc sources, will operate as power sources dependent on the microgrid node voltage (terminal voltage value). The proposed operation range is $430\text{--}465 \text{ V}_{\text{DC}}$ with a linear voltage-to-power behavior. For voltages above $465 \text{ V}_{\text{DC}}$, the power delivered is zero (0%), while for microgrid voltages below $430 \text{ V}_{\text{DC}}$, the output power is maximum (100%). Fig. 2 shows the proposed control law for interlinking converters.

Thus, a DBS linear control law sets the power reference used to generate the output current reference value for the operation of the interlinking converter.

Since there is no voltage loop, the microgrid dc voltage is not directly controlled, but it will be established at the point where the power injected into the microgrid equals the loads’ consumption. Adding more converters in the microgrid does not change the control law. Moreover, an extra power injection (new converter) increases the microgrid dc voltage and, thus, reduces the power delivered by the rest of the converters, leading to a new operating point.

The power converters operating under DBS control must behave as current sources using an internal control loop fed by a current reference. The current compensator processes this reference and provides input for the PWM modulator, thus generating the gate-switching signals. Fig. 3 depicts the control structure proposed for a power converter working under DBS law, in which the DBS control processes the sensed microgrid

node voltage to generate the power reference. The division of the power reference by the measured voltage generates the current reference value. This reference is then limited to the maximum/minimum values the converter accepts and fed to the inner current control loop. The current control allows the converter to operate safely at any output conditions, even under short circuits.

Due to the resistive characteristic of the wires in low-voltage dc microgrids [23], the nodes with a higher load will exhibit a lower voltage. Since DBS establishes a direct relationship between voltage and power, the power-sharing among generators would not be accurate. However, those placed near the higher loads will deliver a more significant amount of power, thus reducing the wiring power losses.

Suppose the full load of a microgrid is concentrated at a point far away from the most powerful converters. In that case, the DBS technique will lead to a poor voltage in the dc bus, exceeding the acceptable voltage deviation limits. Low-bandwidth noncritical communication links can correct this undesirable behavior. However, this is not a realistic scenario since the consumption in a microgrid tends to be distributed, and in most real situations, there is no need for a communication link.

B. Plug-In Electrical Vehicle and Other ESS

Microgrids can lack peak-power capacity under certain circumstances due to their limited number of generators, i.e., during motor start-up or heavy transients in general. The massive integration of plug-in electrical vehicle (PEV) in microgrids is a major challenge due to its high-power demand. Thus, the correct scheduling of its charge/discharge performance is critical for the microgrid's robustness [24].

The microgrid planning classifies the high storage capacity of the PEV as an ESS, which can provide support during heavy power transients. The vehicle-to-grid (V2G) [25] concept states that the charge of the PEV battery must be scheduled according to the microgrid capacity at any moment. Thus, a fully charged battery discharges to support the microgrid, performing as an energy buffer. The integration of the PEV in the grid is studied under the V2G and vehicle-to-building terms [26], [27].

The key point is to charge the battery of the PEV when the microgrid is under low load (i.e., high microgrid voltage, $>460 \text{ V}_{\text{DC}}$); thus, the PEV charging power demand does not affect the microgrid's maximum peak-power capacity. Then, the PEV must be ready to return a portion of its charge to the microgrid if the load approaches the total power capacity on the node of the microgrid (i.e., low microgrid voltage, $<440 \text{ V}_{\text{DC}}$). In the mid-power operation, the PEV battery does not charge/discharge, reserving the available power for the regular microgrid operation.

ESS will work under the control law shown in Fig. 4. A node voltage around the nominal value sets a zero-power reference for ESS. A high voltage value sets a charging current, higher as the microgrid's available power increases. For instance, when a vast amount of PV energy is available in the microgrid. A low voltage value sets a discharging current, higher as the microgrid's available power decreases. The state-of-charge (SoC) of ESS

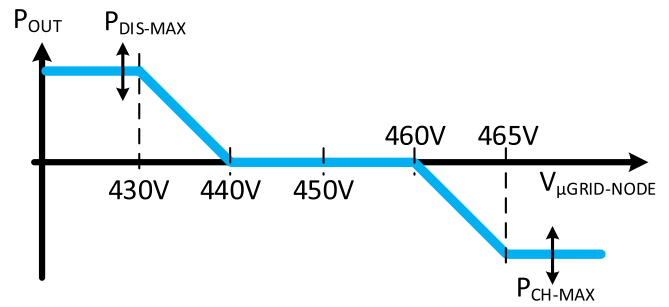


Fig. 4. DBS control law for PEV and ESS.

establishes limits for the maximum current to be supplied/drawn from the battery. Hence, the maximum charge ($P_{\text{ch-MAX}}$) or discharge ($P_{\text{dis-MAX}}$) power of the PEV battery will be adjusted, even dynamically, according to the ESS SoC.

In the case of a full battery, the $P_{\text{CH-MAX}}$ value is set to zero; hence, the converter would not charge the battery. Similarly, below a specific value of SoC, the $P_{\text{DIS-MAX}}$ value is also set to zero, and then the converter would not deliver any energy to support the microgrid.

C. Photovoltaic Energy Sources

Integrating renewable energy sources in microgrids is complicated due to the unpredictable generation and the limited load capacity. Correct microgrid management must ensure that the renewable sources operate at their full available power, feeding the loads and storing the excess energy produced in the ESS systems. When ESS is full, and the load demands less power than those generated by renewable sources, the microgrid must be able to limit the output power of such converters, ensuring a good power quality to the loads. In this research, the dc microgrid integrates PV energy sources.

Small PV power plants are used as low-power distributed energy power sources in most microgrids. Moreover, microgrid management must prioritize the solar energy of a microgrid since its energy source is free, thus lowering the exploitation cost and improving the environmental impact of the microgrid. However, the mismatch between solar energy and power consumption complicates its utilization in microgrids. Thus, coordinating the PV generators with the ESS leads to higher solar energy production.

If the PV generation in a microgrid represents only a tiny percentage of the overall power, the PV generators usually operate at their MPP. As the microgrid demands more power than those produced in the PV generators, there is no need to limit its output. However, when the PV generation reaches high percentages of the installed power, the PV power is expected to exceed the power required by the loads. In such a scenario, the ESS systems must store the excess energy; if it is not possible, the power production must be limited. The proposed DBS law manages loads, ESS, and PV generators.

A PV power converter in a microgrid should behave as follows: running the maximum power point tracking (MPPT) algorithm when the microgrid can absorb the generated power

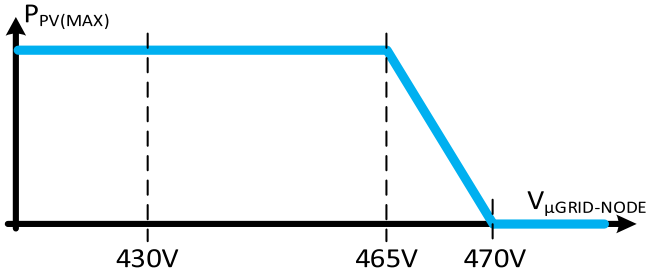


Fig. 5. DBS control law for PV generators.

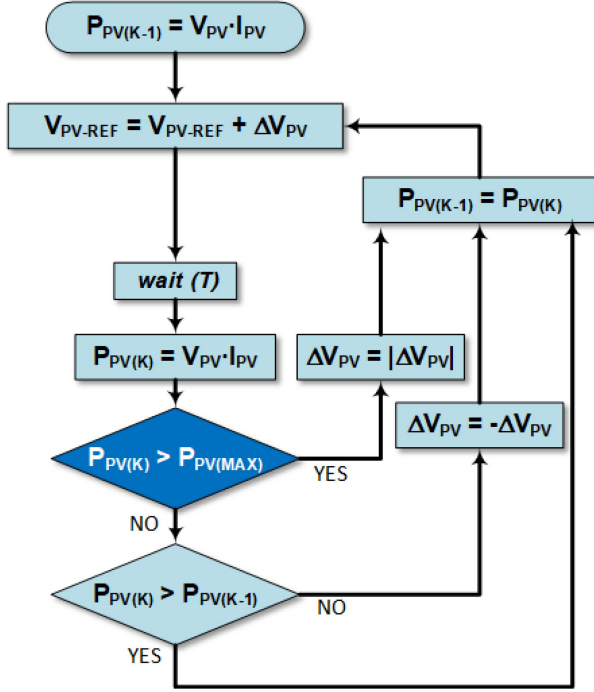


Fig. 6. MPPT algorithm for DBS PV generators.

and limiting the power obtained from the solar modules when the microgrid is not able to absorb it.

In DBS, the microgrid's voltage provides information about the stage-of-load of the microgrid, so it is possible to define some trip voltage values to coordinate and limit the behavior of ESS and PV generators. The trip voltage at which the PV converters limit their output power is set up higher than those for the maximum charging power in the ESS. Hence, the PV converters will operate at the MPP while the ESS charge at their full power capacity if there is excess energy production. When there is no load nor ESS capacity to absorb the PV production, the output power of the PV generators is limited, as depicted in Fig. 5. The slope between 465 V_{DC} and 470 V_{DC} allows equalization of the loads connected to the microgrid and smoothing of transients.

Fig. 6 depicts the MPPT algorithm proposed for the PV generators running under DBS in the dc microgrid. It is based on the classical Perturb&Observe (P&O) method [28]: The voltage reference value is perturbed by a step (ΔV_{PV}), then the system evolves to a new PV voltage value, and the new power

TABLE II
PRIORITY LEVEL FOR LOADS

Microgrid trip voltage	Description
Level 3: non-critical loads ($V > 445 V_{DC}$)	Non-critical loads can be connected when a significant amount of power is available in the microgrid.
Level 2: non-critical loads ($V > 440 V_{DC}$)	Non-critical loads generate only a minor inconvenience if disconnected for some time.
Level 1: critical loads ($V > 435 V_{DC}$)	Critical loads that can be disconnected, if necessary, with a limited inconvenience
Level 0: critical loads ($V > 430 V_{DC}$)	Critical loads that cannot be disconnected from the microgrid. Disconnected only if the microgrid is about to collapse.

is calculated. If the power obtained is increased, the sign of the step is kept; otherwise, it is changed. However, an extra condition has been added ($P_{PV(K)} > P_{PV(MAX)}$) to operate outside the maximum power point (MPP) when the microgrid voltage is higher than 465 V_{DC}. The DBS control law establishes the $P_{PV(MAX)}$ value and limits the maximum power obtained from the PV generator according to the DBS law.

D. Loads

Along with generators and ESS management, load management improves the microgrid robustness against power peaks.

Loads can be classified into critical and noncritical ones. Critical loads must always be powered, while noncritical loads can be disconnected when sufficient power is unavailable in the microgrid's node. Using the DBS technique in each load controller, the status of the microgrid node is estimated, and the load can decide to connect/disconnect.

The microgrid must guarantee enough power to feed the critical loads, traditionally through diesel power generators, running only during critical scenarios. Examples of critical loads are lighting, computers, or medical equipment.

The noncritical loads can be disconnected from the microgrid if the voltage is too low since the microgrid is near to collapse. When the microgrid power capacity increases (for instance, because of a critical-load disconnection), the noncritical loads can be connected again. Examples of noncritical loads are water heaters or air conditioners.

Various priorities for loads can be defined to provide accurate load priority scheduling. The authors propose two levels for critical loads (levels 0 and 1) and two levels for noncritical loads (levels 2 and 3). Table II shows the trip voltages for the different types of loads. A hysteresis of ± 1 V in a V_{DC}-filtered measurement is proposed for stable load connection/disconnection operation.

IV. EXPERIMENTAL RESULTS

A. Microgrid Structure and Equipment

The experimental dc-microgrid used to validate the DBS technique has two nodes with three power converters (overall power of 10 kW), which are connected as shown in Fig. 7.

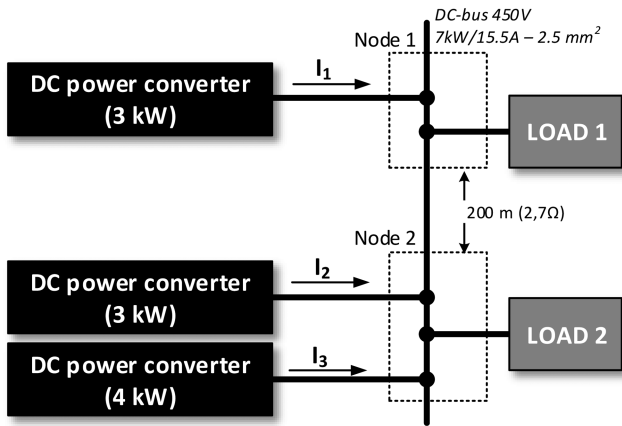


Fig. 7. Physical structure of the tested microgrid.

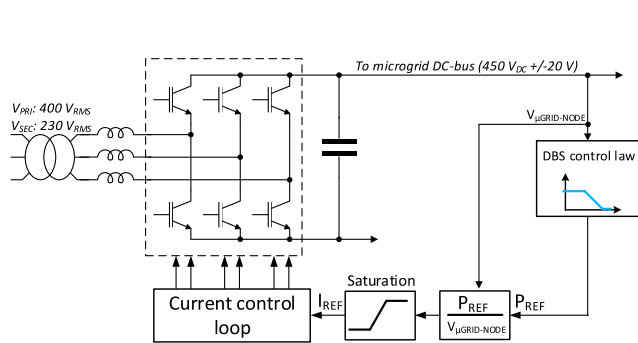


Fig. 8. Interlinking converter: Hardware and control scheme.

Different loads are connected in the nodes. Both converters and loads work according to their terminal's voltage, using the voltage of the microgrid nodes as a microgrid status indicator. The dc-bus is set to $450 V_{DC} \pm 20 V$.

The wire impedance of the power transmission line between nodes #1 and #2 is emulated to provide realistic results. A long line (200 m) of 7 kW (15.5 A/450 V_{DC}) nominal power is supposed. So, the required section in the wiring is 25 mm² (material: aluminum). Since the inductance of an electrical low-voltage transmission line is estimated as 318 μH/km [29], it is neglected in low-voltage microgrids due to its limited length. Generally, in such lines, the inductive part of the impedance is much lower than the resistive one. Hence, a 27 Ω resistor emulates the line impedance.

We have tested three types of converters: interlinking converters, ESS systems, and PV generators. With minimal modifications, the hardware is similar for all of them, adapting the control scheme to the required function. The converters are configured to behave as interlinking converters, PV generators, or ESS as needed for each test. The power stages are three-phase full-bridge topologies designed for a maximum output power of 10 kW but limited to 3 kW/4 kW in the tests that have been carried out. The maximum dc voltage is 750 V.

Interlinking converters are built up by means of a grid-tied three-phase inverter, following Fig. 8. The DBS control law determines the power set point and calculates the current reference.

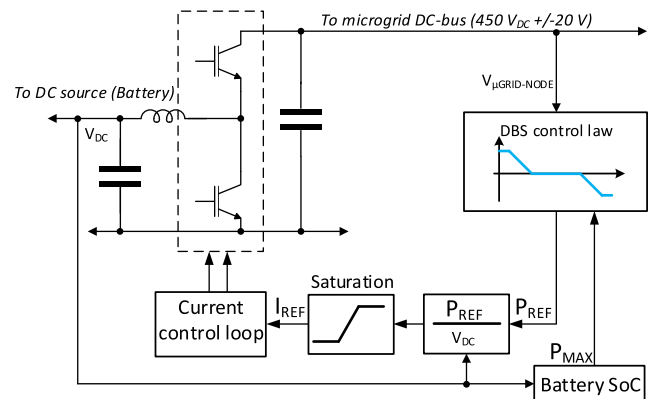


Fig. 9. ESS: Hardware and control scheme.

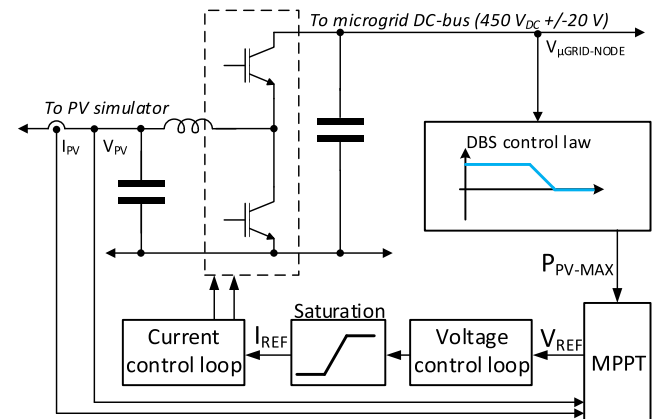


Fig. 10. Solar energy generator: Hardware and control scheme.

Fig. 8 depicts the hardware configuration and the control scheme of this type of agent.

ESS units are built up by using a single leg of the same power stage as for interlinking converters. The measured microgrid dc voltage and the SoC of the battery determines the power set-point, through the DBS control law. Then, the current reference is calculated. The inner current control loop ensures good tracking of such reference. Fig. 9 depicts the hardware configuration and the control scheme of this type of agent.

The solar energy generator is built up by means of the same hardware used for ESS, but the control loops are adapted to the required functionality (see Fig. 10). The measured microgrid dc voltage determines the maximum allowed power. Next, the MPPT algorithm presented in the previous section establishes the voltage reference, and the voltage control loop calculates the current reference. The inner current control loop ensures good tracking of such references. The PV source is emulated by means of a TerraSAS ETS 1000/15 PV simulator, capable of emulating V-I curves and irradiance/temperature dynamic variations.

An electronic load (Chroma 63205A-1200-200) and fixed-value resistors are connected in the nodes to emulate different load transients. A 27 Ω planar resistor emulates the line impedance. Fig. 11 shows the experimental test setup. All the equipment is connected through the experimental microgrid

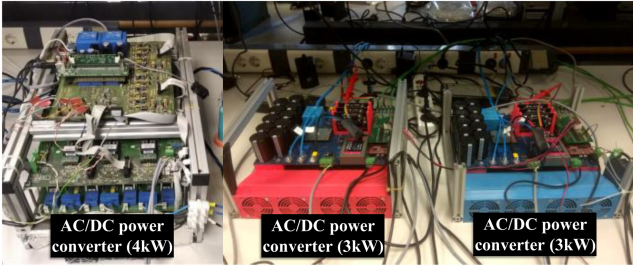
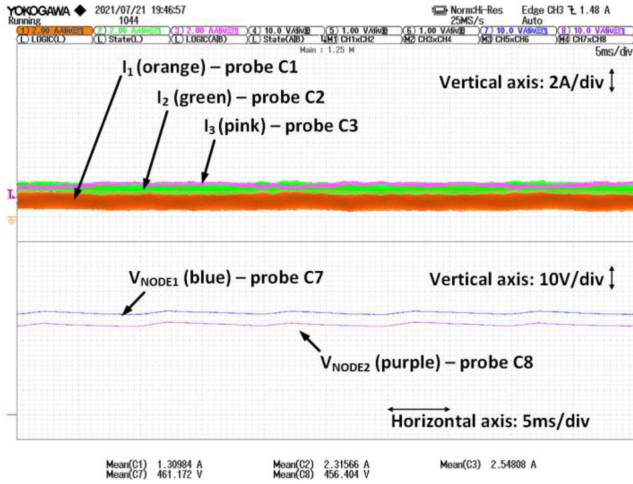


Fig. 11. Experimental setup.

Fig. 12. Microgrid's performance under 30% of the full power (73.3 Ω @node2).

of the Industrial Electronic Systems Group of the Polytechnic University of Valencia, Spain [30]. A set of tests has been carried out showing the performance of the proposed DBS laws.

B. Interlinking Converters (DC Power Sources)

In the first test, the three DC power converters are programmed to behave as interlinking converters with the DBS control law of Fig. 2.

Fig. 12 depicts the stable behavior of the output currents and voltage at the microgrid nodes of the power converters. In this figure, a 27 kW load is connected. Converter #3, connected to the same node as converter #2, delivers a slightly higher current because of its higher power rating. Converter #1, connected to node #1, is far from the load, so its current delivered is lower than those connected near the load (its node voltage is also higher). The power losses in the transmission line (27 Ω) are 46 W. If converters #1 and #2 were fully balanced and delivered the same current as #3, such power losses would be 10.8 W, doubling the inefficiency of the power transmission system.

Fig. 13 depicts the load profile used in the next test. An initial load of 27 kW@450 V_{DC} at node #2 drains the 30% of the full microgrid power. Then, a load of 4 kW at node #1 causes a severe power-up step. After a while, the load at node #1 is disconnected, causing a power-down step.

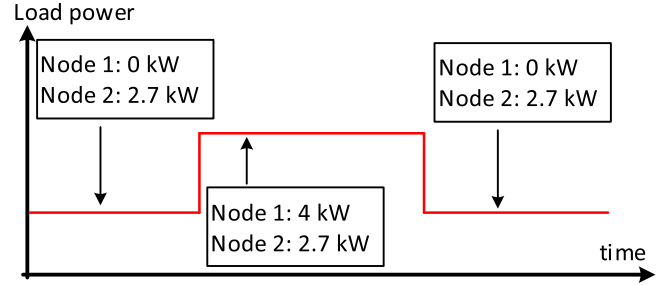


Fig. 13. Load profile for testing DBS dc power sources.

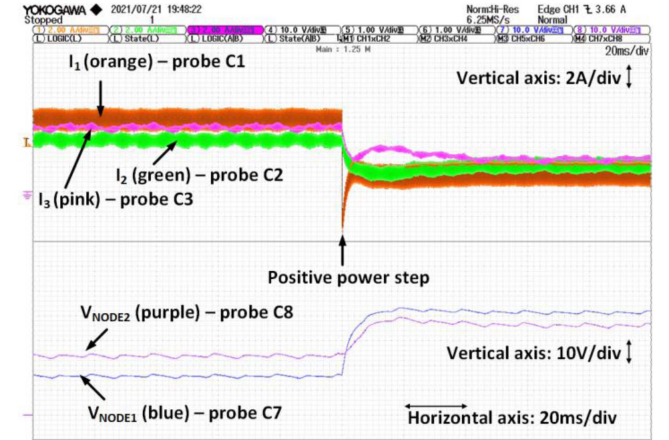


Fig. 14. Positive power step (30%–70% of the full power).

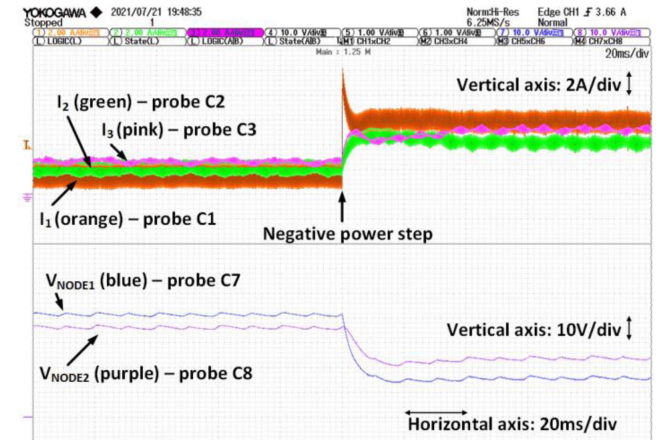


Fig. 15. Negative power step (70%–30% of the full power).

A detailed view of the power transitions (see Figs. 14 and 15) shows how stable and fast the DBS technique works (the voltage transition lasts only 40 ms in both experiments). Note that the current waveforms depicted are the output of the dc power converters, not the inductor current. Hence, the current ripple is due to the output capacitor.

C. PEV and Other ESS

In the second test, the dc power converters #1 and #2 behave as interlinking converters (3 kW each) with the DBS control law from Fig. 2. Converter #3 (4 kW) behaves as an ESS of a PEV,

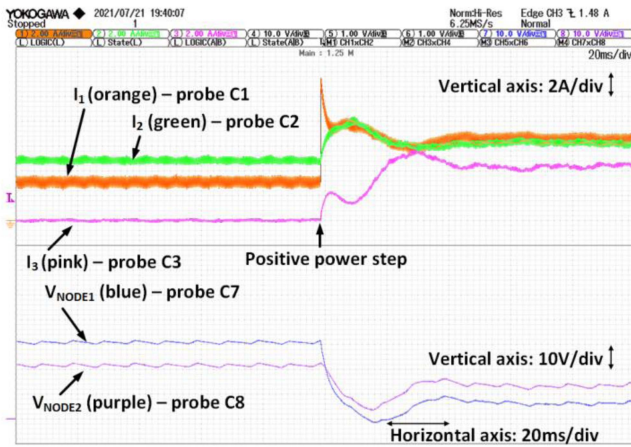


Fig. 16. Positive power step (30%–70% of the full power).

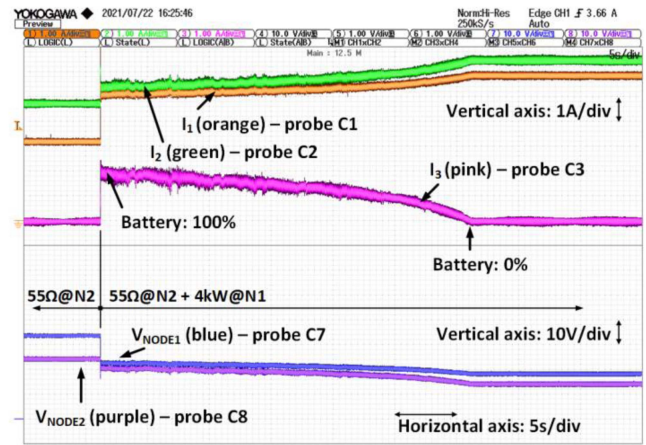


Fig. 18. Battery discharge emulation.

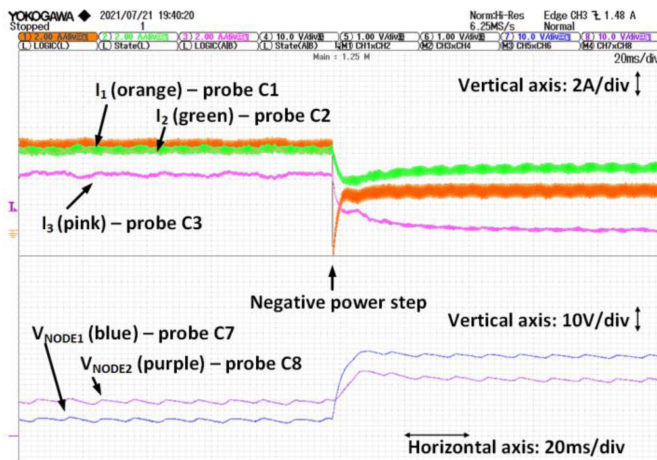


Fig. 17. Negative power step (70%–30% of the full power).

with the DBS control law of Fig. 4. Fig. 13 shows the load profile used, the same as the previous test.

Fig. 16 shows the performance exhibited by the converters. The microgrid loaded to 30% of its total capacity leads to a 441.6 V_{DC} voltage at node #2. Therefore, according to the DBS law depicted in Fig. 4, the ESS (converter #3, pink trace) is idle and does not deliver any power. When the load demand increases, the ESS delivers power to support the microgrid. During the power-up step transient (see Fig. 16), the ESS reaches a steady state operation in less than 60 ms.

At the end of the power-down step transient (see Fig. 17), the ESS returns to an idle state. Both positive and negative voltage and current transients are smooth and stable.

D. PEV and Other ESS Discharge Behavior

Since the batteries are not infinite energy reservoirs, the ESS must deliver less power as time passes and the battery discharges. The ESS is only a transient power support for the microgrid, not a permanent one. In this test, the configuration of the converters is the same as in the previous one, but the ESS converter (converter

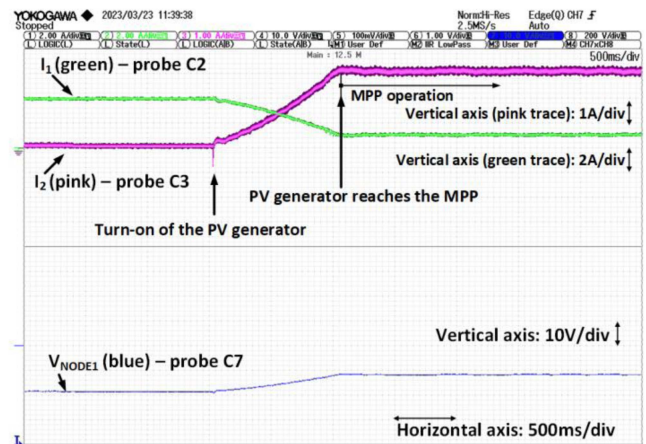


Fig. 19. PV converter operation: Reduction in the power provided by the ESS.

#3) emulates a full discharge from 100% to 0% in 30 s (see Fig. 18).

This test begins with a 37 kW load in node #2, and the ESS does not contribute to supporting the microgrid. Then, the 4 kW resistive load is connected to node 1, and the ESS begins to deliver power to the microgrid. The power provided by the ESS decreases with the SoC of its battery. Once the ESS is empty, converters #1 and #2 must assume the full-load power. The dynamic variation of the maximum power of the ESS shows stable behavior. Integrating this control technique with DBS dc power sources results in a smooth operation.

E. PV Energy Power Converters

A PV generator running the MPPT algorithm under the proposed BDS law feeds the microgrid in this test. Also, a DBS-controlled ESS converter is connected to the microgrid.

First, the PV generator is OFF, and the ESS delivers the full load, green trace (see Fig. 19). The PV generator turns ON at a specific time, and the MPPT algorithm searches for the MPP. Hence, the output current of the PV converter (pink trace) increases up to the maximum value. In this test, the MPPT

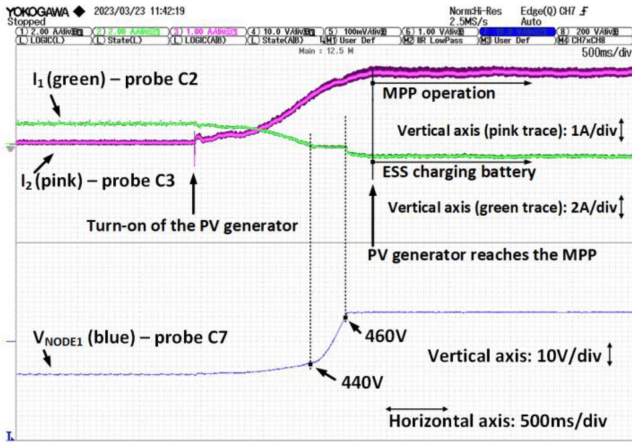


Fig. 20. PV converter operation: ESS changes from delivering power to charging battery mode.

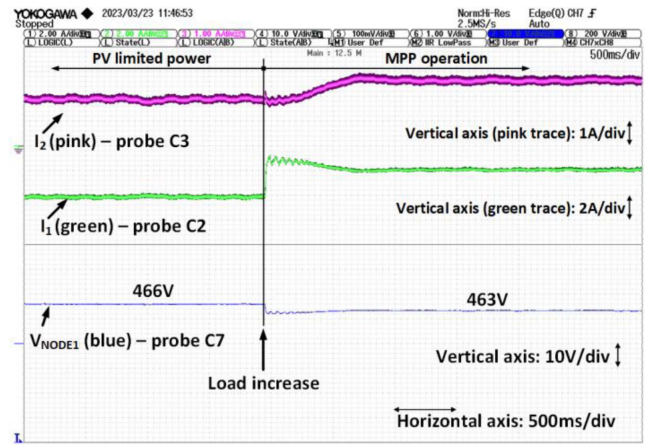


Fig. 22. Increase in the microgrid load, the PV converter can now track the MPP without power constraints.

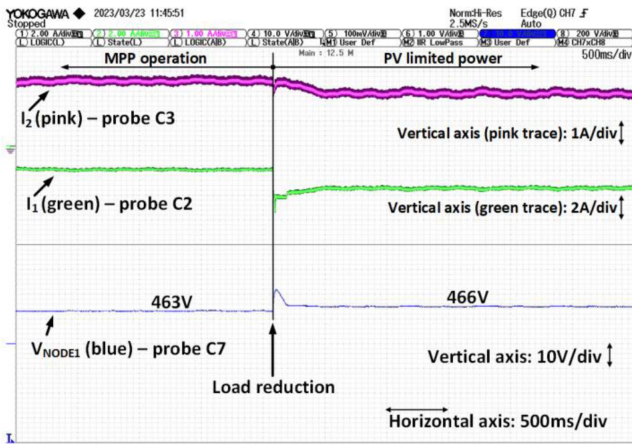


Fig. 21. Load reduction in the microgrid: The PV converter limits its output power, and the ESS charges at full power.

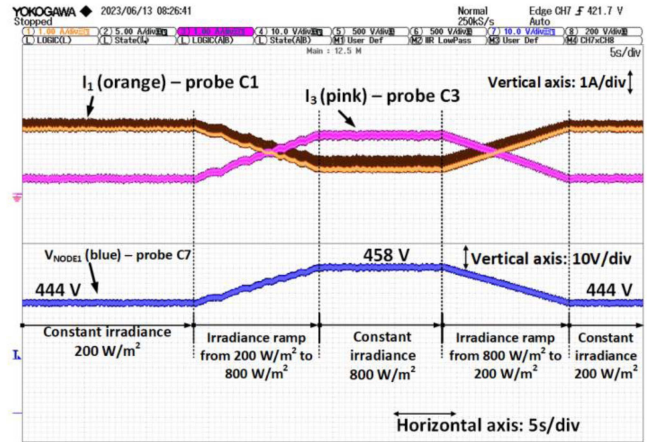


Fig. 23. Irradiance ramp test.

algorithm runs with a PV voltage step of 2.5 V and a running frequency of 10 Hz.

An additional test is performed (see Fig. 20), in which the initial load of the microgrid is lower than in the previous case. As stated before, the PV converter reaches the MPP and the ESS, initially delivering power to the microgrid, switches to the charging battery mode, and drains the excess power between the PV converter and the load consumption.

Fig. 21 shows the behavior of the power limitation of the PV generator. In this test, the load in the microgrid is reduced at a specific time. Hence, the voltage in the microgrid increases (blue trace). Following the DBS control law, the PV generator limits its output power (pink trace), and the ESS increases the charging current to its maximum value (green trace, negative values mean charging current). When the load of the microgrid rises again, the PV converter MPPT algorithm searches for the MPP again without limitations (see Fig. 22).

Additionally, we have tested an irradiance ramp variation. An initial irradiance level of 200 W/m² rises to 800 W/m² at a constant rate in 10 s, then the irradiance level remains constant

for another 10 s; finally, it returns to 200 W/m² with the same slope. Fig. 23 shows the experimental results. As the irradiance increases, the current of the PV generator (pink trace) rises, following the MPP consign. As PV power increases, the power delivered by the interlinking converter (orange trace) is reduced. Thus, following the DBS law, the voltage increases. Consequently, the current delivered by the dc generator decreases. When the irradiance decreases, the PV generator searches for the new MPP, delivering less power and, therefore, the microgrid's voltage decreases. Thus, the interlinking converter delivers more power, following the DBS law.

F. Load Priority Levels

Fig. 24 shows the load priority levels test results using a pair of DBS dc power sources (converters #1 and #2) and an ESS (converter #3). The ESS converter emulates a full battery discharge in 30 s. As in the previous test, the initial load is 37 kW@450 V_{DC} in node #2 (priority level 0), and the ESS is idle. A 24 kW load (priority level 1, must be disconnected at

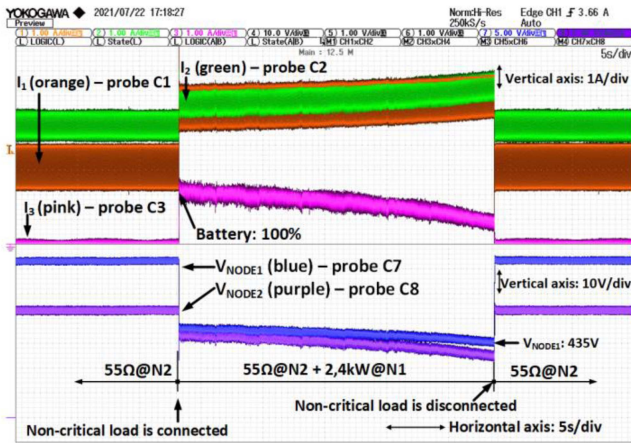


Fig. 24. Load priority levels emulation.

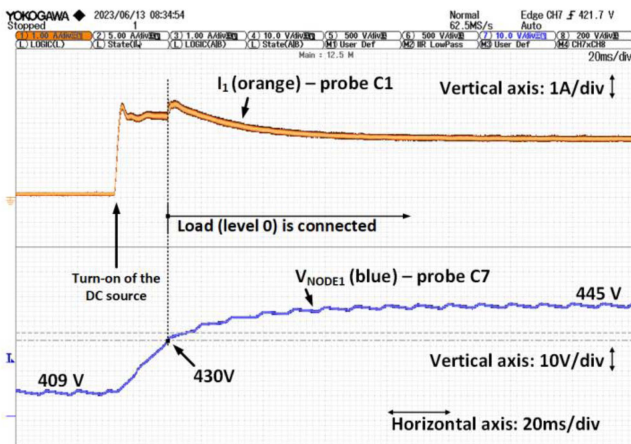


Fig. 25. Example of Microgrid start-up.

voltages lower than $435 V_{DC}$) connects in node #1 at a specific time, and now the ESS delivers power to the microgrid.

As the battery discharges, the ESS reduces its output power. Hence, the power delivered by converters #1 and #2 increases as the voltage decreases. When the voltage at node #1 falls below $435 V_{DC}$, the 24 kW level 1 load self-disconnects and avoids the collapse of the microgrid.

It is worth pointing out that a specific procedure for the microgrid start-up is not needed, due to the following reasons: 1) loads are automatically disconnected when the voltage is insufficient, and 2) converters running the DBS law behave as current sources during the start-up of the microgrid. Despite this, the dc-link capacitors of the converters should be precharged to avoid overcurrents. However, this issue does not concern the operation of the microgrid or DBS, but the converter itself.

To exemplify this, we have carried out a start-up test in which an interlinking converter will supply an initially unpowered microgrid with a critical load (level 0) demanding to be connected.

Initially, the interlinking converter is not running but the dc-link capacitors are precharged through the diodes. In such conditions, the load cannot be fed as the microgrid is unpowered

and there is insufficient voltage. The DBS-controlled interlinking converter is turned on at a specific time, feeding the microgrid, so that the microgrid dc voltage can rise. As soon as the voltage reaches $430 V_{DC}$, the critical load auto connects, and the interlinking converter feeds the required power. Fig. 25 shows the test waveforms for the bus voltage (blue trace) and the current provided by the interlinking converter (orange trace).

V. CONCLUSION

This article presents a control technique for the management of the agents connected to dc microgrids, which is based on DBS. The proposed control law for the different agents in a microgrid (interlinking converters, PV generators, ESS, and loads) fits the agents' requirements and improves the microgrid's robustness.

The integration of renewable energy sources in a microgrid is a major challenge. The operation of a microgrid must guarantee that renewable sources operate at their full available power, using other nonrenewable sources only when sufficient power is not available to supply the loads. When renewable energy sources provide excess power, the microgrid should charge the ESS. This article demonstrates the behavior of a modified P&O algorithm and a DBS law for integrating PV generators in the microgrid. The resulting behavior is satisfactory in harvesting the maximum available power and limiting its production as it is required.

Thus, the use of ESS is a crucial issue in microgrids. These systems improve the harvesting of renewable energy sources, enhance the exploitation cost of the microgrid (stores energy almost for free), and provide stability support.

Moreover, in a low-voltage microgrid, the grid impedance is mainly resistive. Hence, the power-sharing depends on the distance between each converter and the load: the power converters near the load deliver more power than those farther, thus reducing the power losses in the transmission lines.

Tests have been carried out on an experimental microgrid showing satisfactory results, with a smooth transient response for the microgrid dc voltage and good stability. Several combinations of agents have been tested in an experimental dc microgrid performing realistic scenarios. Even the start-up of the microgrid has been tested and demonstrated to be a stable and safe transient.

The proposed DBS technique has proven to be a suitable alternative to coordinate several agents in a microgrid in a robust and stable way, without the need for communication links.

REFERENCES

- [1] D. A. Perez-DeLaMora, J. E. Quiroz-Ibarra, G. Fernandez-Anaya, and E. G. Hernandez-Martinez, "Roadmap on community-based microgrids deployment: An extensive review," *Energy Rep.*, vol. 7, pp. 2883–2898, 2021, doi: [10.1016/j.egy.2021.05.013](https://doi.org/10.1016/j.egy.2021.05.013).
- [2] B. Moran, "Microgrid load management and control strategies," in *Proc. IEEE/PES Transmiss. Distrib. Conf. Expo.*, 2016, pp. 1–4, doi: [10.1109/TDC.2016.7520025](https://doi.org/10.1109/TDC.2016.7520025).
- [3] A. B. Shyam, S. R. Sahoo, and S. Anand, "Voltage regulation and load sharing in DC microgrid using single variable global average estimation," *IEEE J. Emerg. Sel. Topics Ind. Electron.*, early access, Sep. 20, 2023, doi: [10.1109/JESTIE.2023.3317800](https://doi.org/10.1109/JESTIE.2023.3317800).
- [4] Y. Rajbhandari et al., "Load prioritization technique to guarantee the continuous electric supply for essential loads in rural microgrids," *Int. J. Elect. Power Energy Syst.*, vol. 134, 2022, Art. no. 107398, doi: [10.1016/j.ijepes.2021.107398](https://doi.org/10.1016/j.ijepes.2021.107398).

- [5] C. Albea, C. Bordons, and M. A. Ridao, "Robust hybrid control for demand side management in islanded microgrids," *IEEE Trans. Smart Grid*, vol. 12, no. 6, pp. 4865–4875, Nov. 2021, doi: [10.1109/TSG.2021.3101875](https://doi.org/10.1109/TSG.2021.3101875).
- [6] A. Bani-Ahmed, M. Rashidi, A. Nasiri, and H. Hosseini, "Reliability analysis of a decentralized microgrid control architecture," *IEEE Trans. Smart Grid*, vol. 10, no. 4, pp. 3910–3918, Jul. 2019, doi: [10.1109/TSG.2018.2843527](https://doi.org/10.1109/TSG.2018.2843527).
- [7] D. Wang, J. Yang, and S. Lin, "Analysis on transmission characteristics of broadband power line carrier and power frequency integrated communication for new energy microgrid," in *Proc. IEEE 7th Int. Conf. Electron. Inf. Emerg. Commun.*, 2017, pp. 300–303, doi: [10.1109/ICEIEC.2017.8076567](https://doi.org/10.1109/ICEIEC.2017.8076567).
- [8] M. Cintuglu and D. Ishchenko, "Multiagent-based dynamic voltage support of power converters during fault ride-through," *IEEE J. Emerg. Sel. Topics Ind. Electron.*, vol. 3, no. 3, pp. 549–558, Jul. 2022, doi: [10.1109/JESTIE.2021.3119998](https://doi.org/10.1109/JESTIE.2021.3119998).
- [9] G. H. F. Fuzato et al., "Droop K-sharing function for energy management of DC microgrids," *IEEE J. Emerg. Sel. Topics Ind. Electron.*, vol. 2, no. 3, pp. 257–266, Jul. 2021, doi: [10.1109/JESTIE.2021.3074889](https://doi.org/10.1109/JESTIE.2021.3074889).
- [10] H. Beder, B. Mohandes, M. S. E. Moursi, E. A. Badran, and M. M. E. Saadawi, "A new communication-free dual setting protection coordination of microgrid," *IEEE Trans. Power Del.*, vol. 36, no. 4, pp. 2446–2458, Aug. 2021, doi: [10.1109/TPWRD.2020.3041753](https://doi.org/10.1109/TPWRD.2020.3041753).
- [11] J. M. Guerrero, J. C. Vasquez, J. Matas, L. G. de Vicuña, and M. Castilla, "Hierarchical control of droop-controlled AC and DC microgrids—A general approach toward standardization," *IEEE Trans. Ind. Electron.*, vol. 58, no. 1, pp. 158–172, Jan. 2011, doi: [10.1109/TIE.2010.2066534](https://doi.org/10.1109/TIE.2010.2066534).
- [12] S. Sharma, V. M. Iyer, and S. Bhattacharya, "An optimized nonlinear droop control method using load profile for DC microgrids," *IEEE J. Emerg. Sel. Topics Ind. Electron.*, vol. 4, no. 1, pp. 3–13, Jan. 2023, doi: [10.1109/JESTIE.2022.3208513](https://doi.org/10.1109/JESTIE.2022.3208513).
- [13] J. Bryan, R. Duke, and S. Round, "Decentralized generator scheduling in a nanogrid using DC bus signaling," in *Proc. IEEE Power Eng. Soc. Gen. Meeting*, 2004, vol. 1, pp. 977–982, doi: [10.1109/PES.2004.1372983](https://doi.org/10.1109/PES.2004.1372983).
- [14] J. Schonbergerschonberger, R. Duke, and S. D. Round, "DC-bus signaling: A distributed control strategy for a hybrid renewable nanogrid," *IEEE Trans. Ind. Electron.*, vol. 53, no. 5, pp. 1453–1460, Oct. 2006, doi: [10.1109/TIE.2006.882012](https://doi.org/10.1109/TIE.2006.882012).
- [15] F. Li, Z. Lin, Z. Qian, and J. Wu, "Active DC bus signaling control method for coordinating multiple energy storage devices in DC microgrid," in *Proc. IEEE 2nd Int. Conf. DC Microgrids*, 2017, pp. 221–226, doi: [10.1109/ICDCM.2017.8001048](https://doi.org/10.1109/ICDCM.2017.8001048).
- [16] F. Li, Z. Lin, H. Xu, and R. Wang, "A review of DC bus signalling control methods in DC microgrids," in *Proc. IEEE Int. Power Electron. Application Conf. Expo.*, 2022, pp. 1286–1291, doi: [10.1109/PEAC56338.2022.9959577](https://doi.org/10.1109/PEAC56338.2022.9959577).
- [17] J. Schonberger, S. Round, and R. Duke, "Autonomous load shedding in a nanogrid using DC bus signalling," in *Proc. IECON 32nd Annu. Conf. IEEE Ind. Electron.*, 2006, pp. 5155–5160, doi: [10.1109/IECON.2006.347865](https://doi.org/10.1109/IECON.2006.347865).
- [18] C. N. Papadimitriou, V. A. Kleftakis, A. Rigas, and N. D. Hatzigiorgiou, "A DC-microgrid control strategy using DC-bus signaling," *MedPower*, 2014, pp. 1–8, doi: [10.1049/cp.2014.1667](https://doi.org/10.1049/cp.2014.1667).
- [19] K. Sun, L. Zhang, Y. Xing, and J. M. Guerrero, "A distributed control strategy based on DC bus signaling for modular photovoltaic generation systems with battery energy storage," *IEEE Trans. Power Electron.*, vol. 26, no. 10, pp. 3032–3045, Oct. 2011, doi: [10.1109/TPEL.2011.2127488](https://doi.org/10.1109/TPEL.2011.2127488).
- [20] F. Li, Z. Lin, Z. Qian, J. Wu, and W. Jiang, "A dual-window DC bus interacting method for DC microgrids hierarchical control scheme," *IEEE Trans. Sustain. Energy*, vol. 11, no. 2, pp. 652–661, Apr. 2020, doi: [10.1109/TSTE.2019.2900617](https://doi.org/10.1109/TSTE.2019.2900617).
- [21] J. M. Guerrero, M. Chandorkar, T.-L. Lee, and P. C. Loh, "Advanced control architectures for intelligent microgrids—Part I: Decentralized and hierarchical control," *IEEE Trans. Ind. Electron.*, vol. 60, no. 4, pp. 1254–1262, Apr. 2013, doi: [10.1109/TIE.2012.2194969](https://doi.org/10.1109/TIE.2012.2194969).
- [22] I. Patrao, M. Liberos, E. Torán, R. González-Medina, E. Figueres, and G. Garcera, "Coordination of different agents in a microgrid using DC-bus signaling," in *Proc. IEEE 1st Ind. Electron. Soc. Annu. Line Conf.*, 2022, pp. 1–6.
- [23] J. Miret, M. Castilla, and À. Borrell, "Voltage support using electric vehicles in an islanded resistive-microgrid under voltage sags," in *Proc. IEEE 31st Int. Symp. Ind. Electron.*, 2022, pp. 32–38, doi: [10.1109/ISIE51582.2022.9831715](https://doi.org/10.1109/ISIE51582.2022.9831715).
- [24] P. S. Subudhi, S. Padmanaban, F. Blaabjerg, and D. P. Kothari, "Design and implementation of a PV-fed grid-integrated wireless electric vehicle battery charger present in a residential environment," *IEEE J. Emerg. Sel. Topics Ind. Electron.*, vol. 4, no. 1, pp. 78–86, Jan. 2023, doi: [10.1109/JESTIE.2022.3195087](https://doi.org/10.1109/JESTIE.2022.3195087).
- [25] Y. Shen, T. He, D. Liu, Y. Tang, and Y. Wang, "e-CNY vehicle-to-grid real-time settlement system," *IEEE J. Emerg. Sel. Topics Ind. Electron.*, early access, Aug. 9, 2023, doi: [10.1109/JESTIE.2023.3303833](https://doi.org/10.1109/JESTIE.2023.3303833).
- [26] C. Pang, P. Dutta, and M. Kezunovic, "BEVs/PHEVs as dispersed energy storage for V2B uses in the smart grid," *IEEE Trans. Smart Grid*, vol. 3, no. 1, pp. 473–482, Mar. 2012, doi: [10.1109/TSG.2011.2172228](https://doi.org/10.1109/TSG.2011.2172228).
- [27] Z. Wang and S. Wang, "Grid power peak shaving and valley filling using vehicle-to-grid systems," *IEEE Trans. Power Del.*, vol. 28, no. 3, pp. 1822–1829, Jul. 2013, doi: [10.1109/TPWRD.2013.2264497](https://doi.org/10.1109/TPWRD.2013.2264497).
- [28] D. Routray, P. K. Rout, and B. K. Sahu, "A brief review and comparative analysis of two classical MPPT techniques," in *Proc. Int. Conf. Adv. Power. Signal, Inf. Technol.*, 2021, pp. 1–6, doi: [10.1109/AP-SIT52773.2021.9641301](https://doi.org/10.1109/AP-SIT52773.2021.9641301).
- [29] "Technical guide for application of the low-voltage electrical regulation in Spain (in Spanish)," 2003. Accessed: Mar. 25, 2023. [Online]. Available: <https://industria.gob.es/Calidad-Industrial/seguridadindustrial/instalacionesindustriales/baja-tension/Paginas/guia-tecnica-aplicacion.aspx>
- [30] R. Salas-Puente, S. Marzal, R. González-Medina, E. Figueres, and G. Garcera, "An algorithm for the efficient management of the power converters connected to the DC bus of a hybrid microgrid operating in grid-connection mode," *Electric Power Compon. Syst.*, vol. 46, no. 9, pp. 1029–1043, May 2018, doi: [10.1080/15325008.2018.1469177](https://doi.org/10.1080/15325008.2018.1469177).



Iván Patrao received the M.Sc. degree in Ingeniero Industrial and Ph.D. degree in electrical engineering from the Polytechnic University of Valencia (UPV), Valencia, Spain, in 2009 and 2015, respectively.

In 2008, he was with the R&D Department of Siliken, involved in the design of electronic systems applied to photovoltaic applications. Since 2009, he has been with the Industrial Electronics Systems Group, Electronics Engineering Department, UPV, where he is an Assistant Professor. His research interests include power converter modeling and control, converters for renewable energy, transformerless inverters, and integration of distributed energy sources in microgrids.



Enric Torán received the Ingeniero Industrial (M.Sc.) and the Electronic Systems Engineering (M.Sc.) degrees in 2019 and 2020, respectively, from the Universitat Politècnica de València (UPV), Valencia, Spain, where he is currently working toward the Ph.D. degree in electrical engineering with focus on converters connected to very weak grids and improving the grid quality.

Since 2021, he is with the Industrial Electronics Systems Group (GSEI), Electronics Engineering Department, UPV, where he researches in power converters, microgrids, and converters for renewable energy sources.



Raúl González-Medina was born in Valencia, Spain, in 1978. He received the Ingeniero Industrial (M.Sc.) degree and the Ph.D. degree in electrical engineering from the Universidad Politécnica de Valencia (UPV), Valencia, Spain, in 2005 and 2015, respectively.

In 2005, he joined the Department of Electronics Engineering, UPV, where he is currently an Associate Professor of power electronics. He is also involved with the Industrial Electronic System Group. His main research interests include power converters, modulation techniques, grid-connected inverters, and converters for renewable energy sources.



Marian Liberós was born in Valencia, Spain, in 1992. She received the master's (M.Sc.) degree in electronic systems engineering and the Ph.D. degree in the doctoral programme in electronic engineering from the Universitat Politècnica de València (UPV), València, Spain, in 2016 and 2021, respectively.

She is an Assistant Professor with the UPV. Since 2015, she is with the Industrial Electronic System Group, where she researches in power converters, circulating currents in converters connected in parallel, and active filters.



Emilio Figueres (Senior Member, IEEE) received the M.Sc. degree from Ecole Nationale Supérieure d'Electrotechnique, d'Electronique, d'Informatique et d'Hydraulique de Toulouse, Toulouse, France, in 1995, and the Dr. (Ingeniero Industrial) (Ph.D.) degree from Universitat Politècnica de València (UPV), València, Spain, in 2001.

Since 1996, he has been with the Electronics Engineering Department, UPV, where he is currently a Full Professor and was the Head of the Department from 2008 to 2016. Since 2005, he has been responsible for the UPV Ph.D. Program in electronics engineering. He holds seven patents about power electronics, five of them licenced by industrial companies. He has authored or coauthor more than 100 papers published in JCR-indexed journals and international conferences on power electronics and renewable energy. His research interests include power processing of renewable energy sources, microgrids, grid connected converters, and power management in electric vehicles, working closely with industry on these topics through more than 30 company-funded research contracts.

Mr. Figueres is the co-recipient of the best paper award at the IEEE INDUSTRIAL ELECTRONICS TRANSACTIONS in 2012.



Gabriel Garcerá (Senior Member, IEEE) received the Ph.D. degree in electrical engineering from the Universitat Politècnica de València (UPV), València, Spain, in 1998.

He is currently a Full Professor of power electronics with UPV. He has authored or coauthored more than 100 papers about his reserch interest topics in international journals and conferences, having advised 16 Ph.D. Thesis. He has been working in more than 50 research projects with companies and academia, many of them dealing with photovoltaic

power converters. His main research interests include power electronics and its applications to renewable energy, distributed generation microgrids and electric vehicles.

Dr. Garcerá was an Associate Editor of IEEE TRANSACTIONS ON INDUSTRIAL ELECTRONICS from 2004 to 2019.